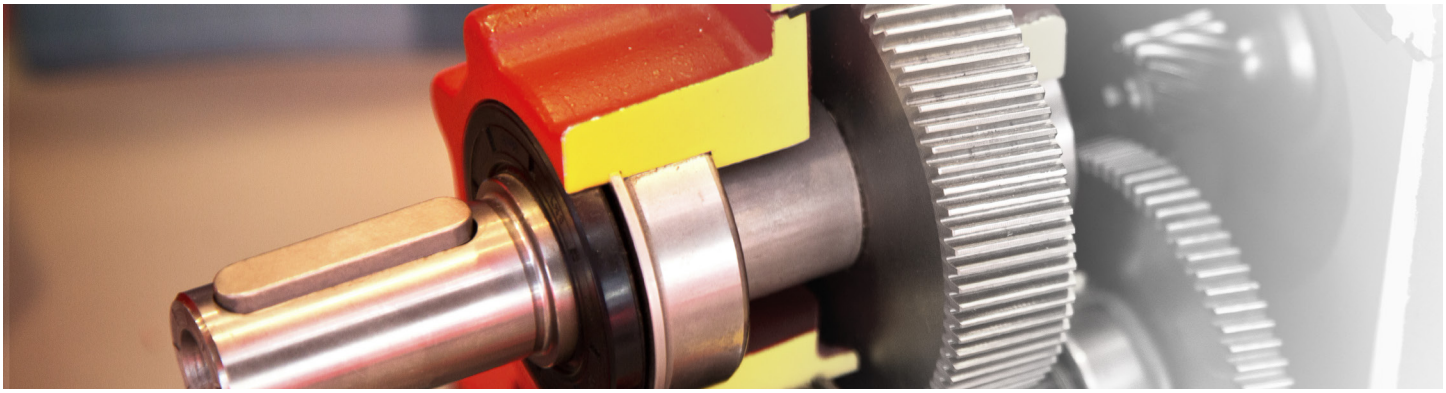

WHITE PAPER | #X1

VIBRATION MONITORING OF GEARBOXES

Written By
James C. Robinson,
Technical Consultant, IMI division of PCB Piezotronics

Curated By
Meredith Christman,
Product Marketing Manager, IMI division of PCB Piezotronics

VIBRATION MONITORING OF GEARBOXES

Article by:
James C Robinson, Technical Consultant, IMI division of PCB Piezotronics

Curated by:
Meredith Christman, Product Marketing Manager, IMI division of PCB Piezotronics

INTRODUCTION

Gearboxes are a common component in many industries, including chemicals, sugar, steel, mining, plastics, oil & gas, power and petrochemical. Because their operation is essential to many manufacturing processes, planned downtime is inconvenient and unplanned downtime can be catastrophic.

The objective of this paper is to demonstrate a wide variety of fault types and the importance of employing proper sensors and analysis tools. Particular emphasis is placed on vibration monitoring employing accelerometers as sensors on industrial gearboxes.

SECTION 1: SENSOR SELECTION AND MOUNTING

Potential Faults of Gearboxes: Prior to selecting sensors and addressing their mounting on a gearbox, it will first be beneficial to remind ourselves of the characteristics of the vibration signature that can be expected from common gearbox faults. For example, if there is a crack in a gear, it will likely introduce a slight speed change when the defective tooth enters the load zone. This leads to impacting every time that tooth enters into its load carrying responsibility (typically once per revolution of that gear). Now consider a situation where there is a lack of sufficient lubrication for the gear teeth going into and out of the load zone. This leads to friction between the teeth with the maximum activity typically occurring twice per tooth mesh (once on the addendum and once on the dedendum). Of course, both friction and impacting can also occur within the gearboxes. In gearboxes, impacting will generally be periodic and friction generally non-periodic (random).

If a fault is present that is generating stress wave activity on a set of meshing gears, that energy will be transmitted to the outer housing via the shafts where the gear set is attached through the bearings (providing they are rolling element bearings). An accelerometer fastened to the outer surface in the proximity of that bearing would capture the stress wave activity providing the accelerometer has sufficient bandwidth and sensitivity. If the bearing is a sleeve bearing, significant attenuation will occur to the stress waves in coupling across the gap from inner race to outer race and thus may not be sufficient for capture by the sensor. A proximity probe lacks sufficient sensitivity for the relatively high frequency stress wave activity.

In addition to the relatively high frequencies present in the stress wave packets generated by friction and impacting, the lower frequencies generated by faults such as misalignment, looseness and balancing issues must also be captured and analyzed. These stress wave packets contain frequencies in one of the following two ranges:

- About 0.3 times running speed to about 3.25 times the gear meshing frequency.
- About 0.3 times running speed to about 50 times running speed.

The analysis of the low-frequency band is carried out by capturing a time waveform and proceeding to transform that time waveform into spectra data on which most of the diagnostics are carried out. For the high-frequency band, the most common procedure is to run the signal from the sensor through a high-pass filter followed by full-wave rectification. The rectified signal is then demodulated to extract any periodic or random

activity that is occurring. If periodic or random activity is occurring, the analyst needs to know the periodic rate as well as the amplitude of the activity. Classic demodulation techniques do not maintain the true g-level. The cases presented in this paper use the PeakVue™ methodology developed by Emerson Process Management, which does maintain the true peak g-level.

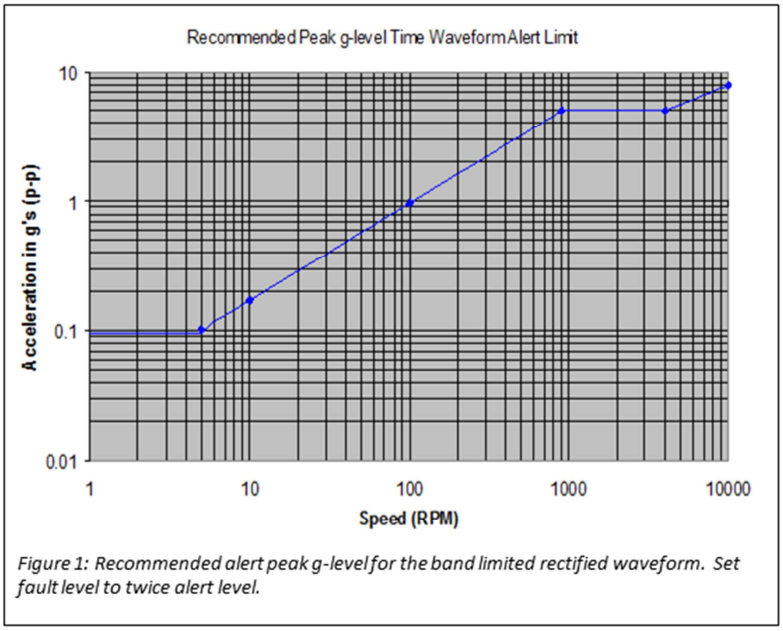

Figure 1: Recommended alert peak g-level for the band limited rectified waveform. Set fault level to twice alert level.

When the analyst does find a fault in a piece of equipment and reports it to operations, the typical response from operations is to ask about the severity of the fault and how long can the equipment continue to operate. These questions sometimes are difficult to answer. For the low-frequency band data, there are several charts available in the industry that can be used to make intelligent judgment calls on both fault severity and continued equipment operation. For the high-frequency band, assuming the true peak acceleration level and speed (RPM) are available, the chart in Figure 1 has been created to provide similar intelligent answers on both fault severity and continued equipment operation. The level given in the chart is the recommended alert level; the recommended fault level is twice the alert level.

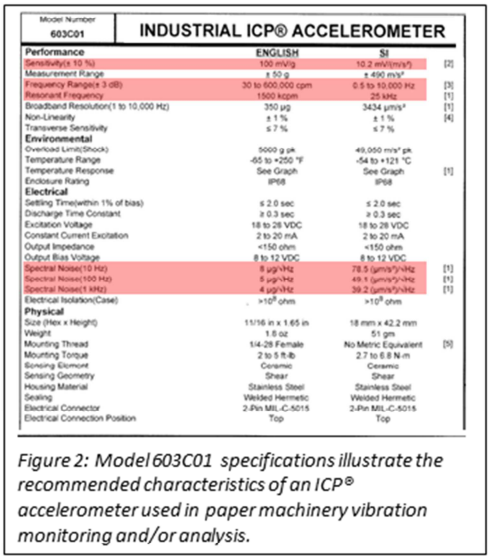

Model Number 603C01	INDUSTRIAL ICP® ACCELEROMETER	
Performance	**ENGLISH**	**SI**
Sensitivity(± 10 %)	100 mV/g	10.2 mV/(m/s²)
Measurement Range	± 50 g	± 490 m/s²
Frequency Range(± 3 dB)	30 to 600,000 cpm	0.5 to 10,000 Hz
Resonant Frequency	1500 kcpm	25 kHz
Broadband Resolution(1 to 10,000 Hz)	350 µg	3434 µm/s²
Non-Linearity	± 1 %	± 1 %
Transverse Sensitivity	≤ 7 %	≤ 7 %
Environmental		
Overload Limit(Shock)	5000 g pk	49,050 m/s² pk
Temperature Range	-65 to +250 °F	-54 to +121 °C
Temperature Response	See Graph	See Graph
Enclosure Rating	IP68	IP68
Electrical		
Settling Time(within 1% of bias)	≤ 2.0 sec	≤ 2.0 sec
Discharge Time Constant	≥ 0.3 sec	≥ 0.3 sec
Excitation Voltage	18 to 28 VDC	18 to 28 VDC
Constant Current Excitation	2 to 20 mA	2 to 20 mA
Output Impedance	<150 ohm	<150 ohm
Output Bias Voltage	8 to 12 VDC	8 to 12 VDC
Spectral Noise(10 Hz)	8 µg/√Hz	78.5 (µm/s²)/√Hz
Spectral Noise(100 Hz)	5 µg/√Hz	49.1 (µm/s²)/√Hz
Spectral Noise(1 kHz)	4 µg/√Hz	39.2 (µm/s²)/√Hz
Electrical Isolation(Case)	>10⁸ ohm	>10⁸ ohm
Physical		
Size (Hex x Height)	11/16 in x 1.65 in	18 mm x 42.2 mm
Weight	1.6 oz	51 gm
Mounting Thread	1/4-28 Female	No Metric Equivalent
Mounting Torque	2 to 5 ft-lb	2.7 to 6.8 N-m
Sensing Element	Ceramic	Ceramic
Sensing Geometry	Shear	Shear
Housing Material	Stainless Steel	Stainless Steel
Sealing	Welded Hermetic	Welded Hermetic
Electrical Connector	2-Pin MIL-C-5015	2-Pin MIL-C-5015
Electrical Connection Position	Top	Top

Figure 2: Model 603C01 specifications illustrate the recommended characteristics of an ICP® accelerometer used in paper machinery vibration monitoring and/or analysis.

ICP® Accelerometer Use: The most common sensor type employed in vibration analysis on gearboxes are ICP® accelerometers with a sensitivity of 100 mV/g, a resonant frequency in the 25 kHz range and a noise floor of approximately 100 µg/√Hz at 1 Hz (or less). IMI Model 603C01 (top exit with ¼-28 female mounting thread) would be an example of an ideal model. The specification sheet for the accelerometer typically specifies the sensitivity is nominally flat to within 3dB from a fraction of 1 Hz to 10 kHz. See Figure 2 for an example of the characteristic compliance of Model 603C01.

The implicit assumption is that the sensor is attached to a clean flat surface with a stud at a specified torque. Because stud mounting is both expensive and time consuming, its requirement encourages sparse data acquisition. The analyst will often turn to a much simpler means of attaching the sensor to the surface, such as using a two-rail magnet placed on a curved surface with the sensor attached to the magnet. This approach will often lead to not capturing the higher frequencies associated with impacting or friction.

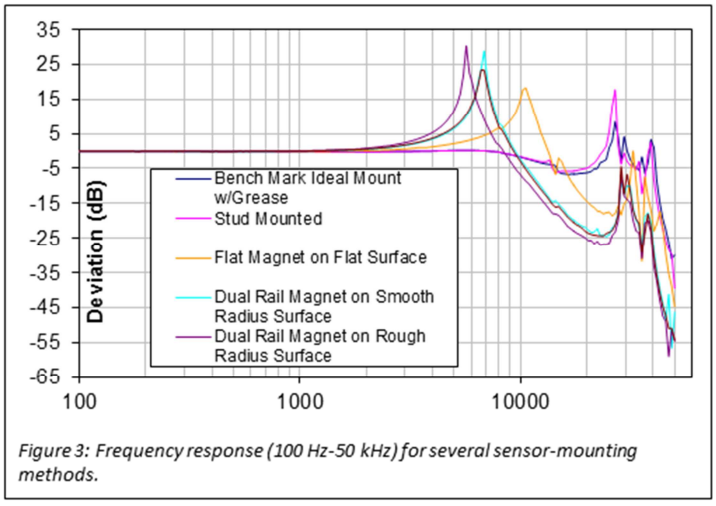

Figure 3: Frequency response (100 Hz-50 kHz) for several sensor-mounting methods.

To explore the impact that sensor mounting has on the sensor frequency response, frequency response data was captured (presented in Figure 3) for a sensor that was:

- Mounted with a stud with grease on a flat dry surface.
- Mounted with a stud without grease on a flat dry surface.
- Mounted with a flat magnet on a flat clean surface.
- Mounted with a dual-rail magnet mounted on smooth curved surface.
- Mounted with a dual-rail magnet mounted on rough curved surface.
- Mounted with a dual-rail magnet mounted on painted curved surface.

For faults that manifest themselves in the frequency range of less than 2 kHz such as alignment, unbalance and looseness, the results would be independent of how the sensor is mounted. For faults identified with higher frequencies (impacting and friction), the results would be highly dependent to how the sensor is mounted ranging from no response to distorted response.

Of course, the best way to mount would be stud-mount with a specified torque. This could get expensive as it requires a dedicated accelerometer at every measurement point. An acceptable alternative mounting would be to use a flat magnet placed on a flat smooth surface such as a mounting pad. The flat magnet approach to all measurements points combined with stud mounting the sensor in radial direction on the inboard and outboard ends would be a recommended method for sensor mounting.

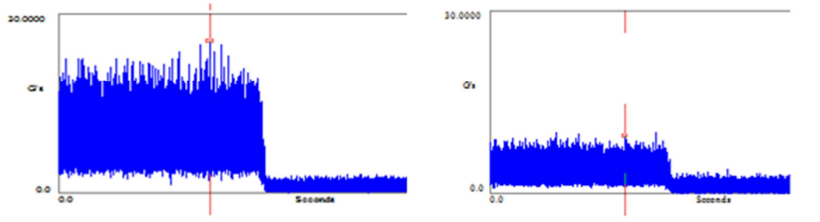

Figure 4: The lefthand time trace is for an accelerometer mounted with a flat magnet attached to a mounting pad. The righthand time trace is for an accelerometer attached to a dual rail magnet set on a curved surface. Grease introduced into the bearing at the time both sensors dropped in magnitude. The 25 g's in the lefthand time trace is considered to be serious (well above fault level presented in Figure 2) while the 9.5 g's in the righthand time trace would be considered as "action is required in near future" but just now entering the fault level as defined. (The higher g level in the lefthand time trace instills a sense of immediate action is needed).

To illustrate the type of effect that sensor mounting can have on friction activity, data is presented in Figure 4 from a case where it was known that bearing lubrication was needed. In the lefthand time trace, the sensor was mounted using a flat magnet attached to a flat smooth surface. A second set of data on the righthand time trace was acquired from a sensor attached to a curved surface via a dual-rail magnet. Both time traces were taken at the same time using a two-channel data collector. The bearing was lubricated (greased) at the time the sudden level of noise decreased.

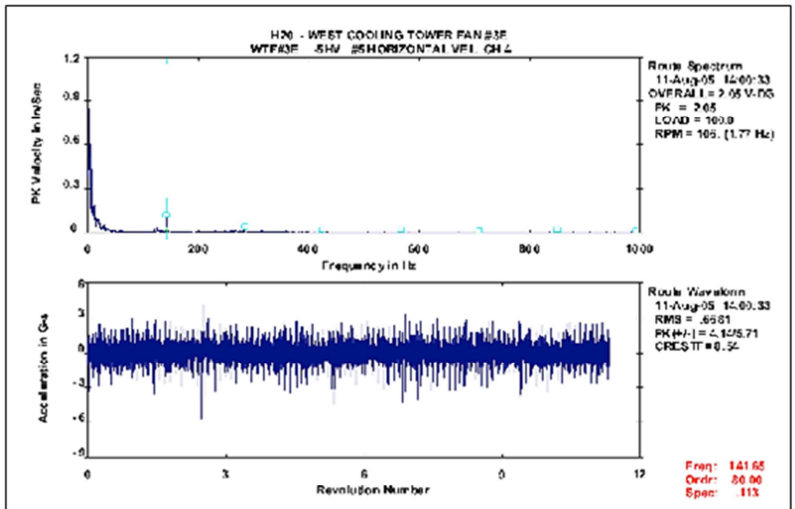

Figure 5: Velocity spectral data and waveform acquired from cooling tower gearbox with 100 mV/g sensor after restart of reassembled gearbox.

SECTION 2: COOLING TOWER GEARBOX

A metals plant lost the use of one of its cooling towers due to a two-speed gearbox becoming unusable. The gearbox replacement had a long lead-time but sufficient parts were available to put together a temporary gearbox replacement. When the cooling tower was placed back in service with the temporary gearbox at low speed, vibration velocity spectral data was

acquired and is presented in Figure 5. The peak-to-peak g-level is less than 10 g's, and the spectral data is a "ski slope". This is typical for an ICP® accelerometer that is being overloaded. The sensor was a 100 mV/g accelerometer with a 9-11 VDC bias voltage.

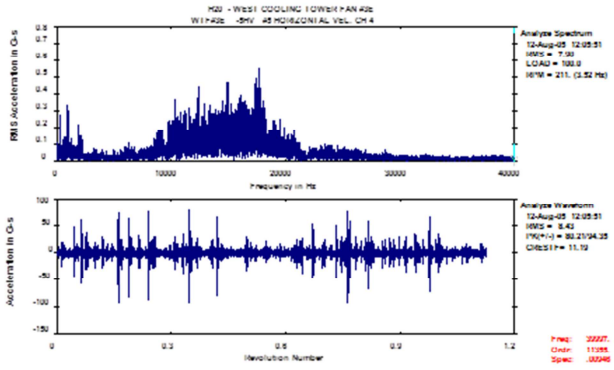

Figure 6: Acceleration spectra data and waveform acquired with the 10 mV/g sensor.

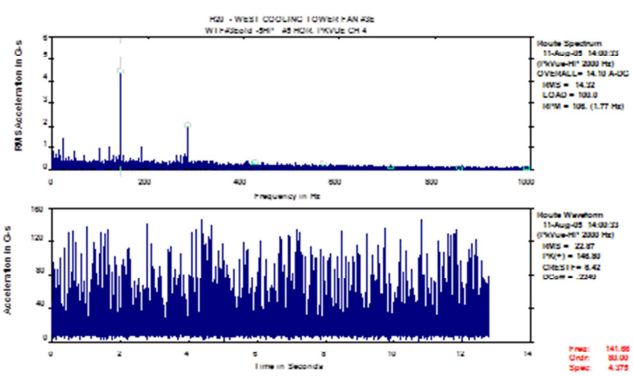

Figure 7: High-frequency band activity from the cooling tower gearbox with gearbox running on low speed.

The accelerometer was replaced with a 10 mV/g accelerometer with a similar bias voltage. Using the 10 mV/g sensor, a 40 kHz acceleration spectra data set with waveform was captured and is presented as Figure 6. The peak-to-peak g-level was close to 200 g's, explaining why the 100 mV/g sensor's output was unstable. The primary cause of the high g-levels was friction occurring within the bearings as well as between the gear teeth as a result of an inoperable lubrication system driven by a gear oil pump.

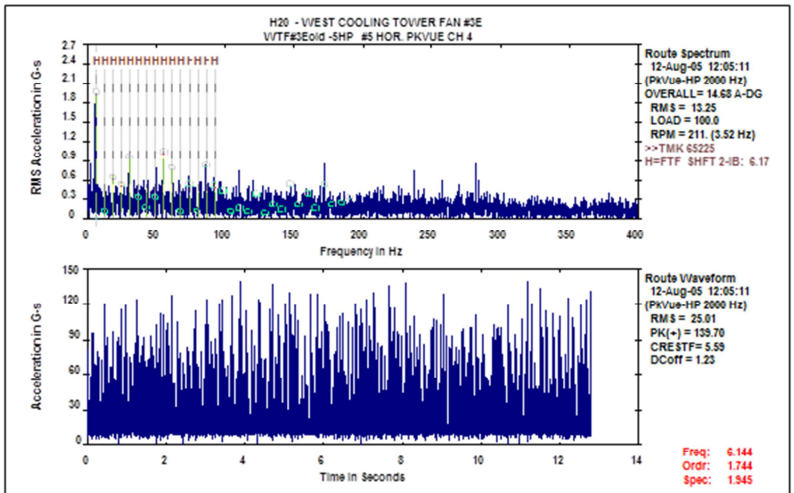

Figure 8: High-frequency band activity from the cooling tower gearbox with gearbox running on high speed.

The operators chose to continue operating the cooling tower rather than take the time to correct the lubrication problem. They did ask the analyst if it would be best to run the gearbox at high speed or at low speed. It was decided to run high-frequency analysis at both speeds to see if the best speed could be determined from the data. The high-frequency band chosen for the analysis was 2-40 kHz. The results for the gearbox running at high speed are presented in Figure 7. There was significant periodic activity at one and two times gear mesh frequency. The peak g-level in the waveform is 150 g's, which is very high. The results for the gearbox running at low speed are presented in Figure 8. The significant difference between the high-speed and low-speed activity is the lack of any gear mesh frequency or twice gear mesh frequency activity in the high-speed data relative to the low-speed data. The peak g-level in the high-speed data is 140 g's, which is slightly lower than the peak g-level of 150's in low-speed data. The presence of the gear mesh frequency and twice gear mesh frequency in the low-speed data suggests that debris from the friction between gear teeth was being thrown out into bearings. The conclusion was that there was sufficient oil in the bottom of the gearbox to permit the gear to sling oil out to lubricate the gear teeth when running at high speed. Therefore, it was decided that less damage would occur with the gearbox running at high speed. The gearbox was run at high speed until replaced with the new gearbox.

SECTION 3: MULTI DRILL HEAD GEARBOX

Vibration measurements were taken on several multi drill head gearboxes at an automobile transmission plant. The primary objective was to demonstrate that vibration analysis of the high-frequency band could reliably detect early-stage bearing faults in drill heads. In addition to bearing faults, several other faults were found. One of those other faults was a torsional vibration problem on a particular gearbox with ten drill heads. The gear arrangements were accomplished with the two levels depicted in Figure 9. Assuming the two-pole motor was running with no slip (3,600 RPM or 60 Hz), the gear mesh frequency for the level 1 gear set is 2,280 Hz. Three times gear mesh frequency is 6,840 Hz, thus the use of a low-frequency bandwidth of 20-8,000 Hz was most appropriate. There are possibly three additional gear mesh frequencies associated with the gear configurations in the level 1 configuration presented in Figure 9. The gear mesh frequency for the cluster of gears driven by I-1 is 2,146 Hz. The other two gear set clusters driven by I-3 and I-4 are 2,280 Hz.

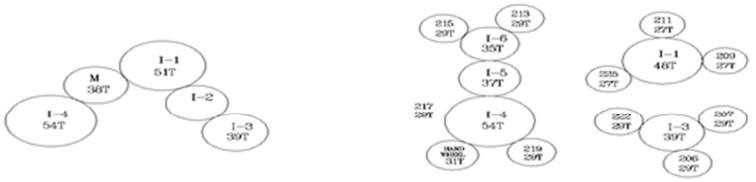

Figure 9: Two level gear arrangements for the ten-drill head gearbox. Level 1 is illustrated on the right while Level 2 is illustrated on the left. The ten drill heads are identified as 213, 215, 217, 219, 206, 207, 209, 211, 225 and 222.

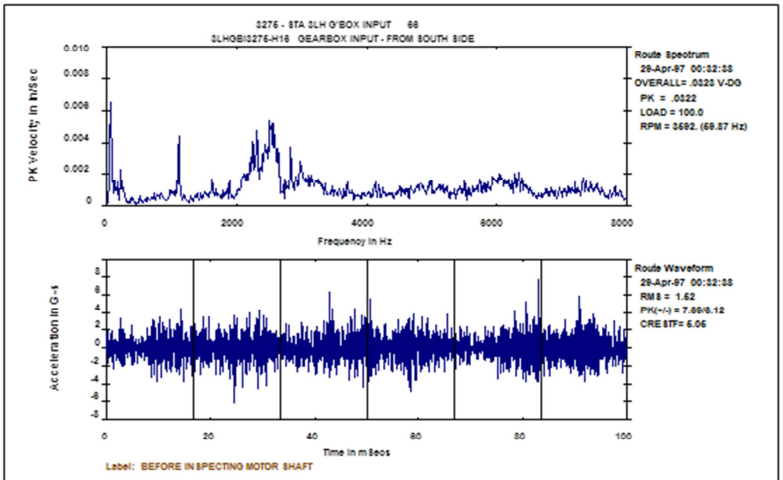

Figure 10: Low-frequency band spectra and waveform data pre motor shaft inspection.

The low-frequency band spectra and waveform data are presented in Figure 10. The peak-to-peak g-level in the waveform data is about 14 g's. There is definite periodic activity around 1,000 Hz. There are probably two individual gear mesh frequencies in the expected frequency range of 2,100 to 2,300 Hz. Additionally, there is a broad band of spectra activity in the 2,500 to 2,800 Hz frequency range. The high-frequency (5 to 40 kHz) rectified waveform and spectra data taken at the same time as the low-frequency band data are presented in Figure 11. The spectra bandwidth of the high-frequency data in Figure 11 was specified at 1,000 Hz, which was an oversight. It should be slightly greater than twice gear mesh frequency (5 kHz). The peak g-level in the rectified waveform is about 8 g's. The bothersome feature of concern in the high-frequency spectra data in Figure 11 is the activity at slightly greater than 0.5 times running speed. It is an indication of a possible torsional resonance. Based on this observation, it was decided to inspect the motor shaft/key. A picture of the motor shaft/key is presented in Figure 12. There

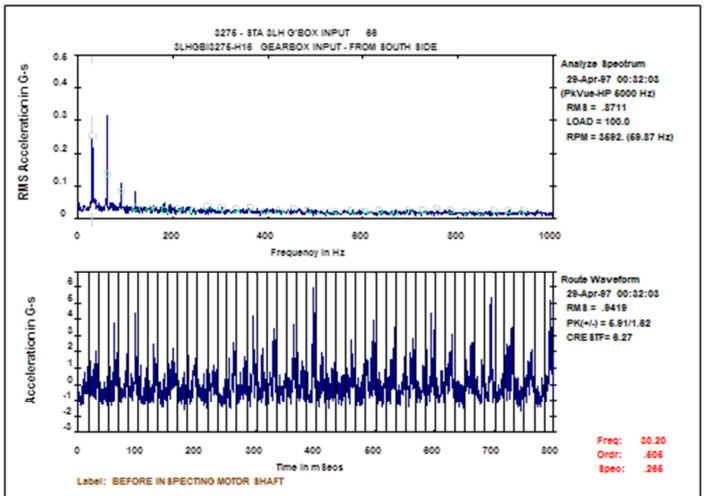

Figure 11: High-frequency band (5 kHz to 40 kHz) PeakVue spectra and waveform data pre motor shaft inspection. Note the periodic activity.

Figure 12: Picture of shaft from motor showing the shaft keyway wear.

has been considerable wear in the motor shaft keyway. The recommended solution was to decrease the tolerances in the keyway fit to the shaft. This corrected the shaft/key wear problem.

Spectra data taken after the motor shaft replacement is presented in Figures 13 and 14. The resolution is sufficient to clearly show the gear mesh frequency at 2,275 Hz as well as a probable torsional resonance at a frequency slightly greater than gear mesh frequency. The periodic activity that was seen in the high-frequency rectified waveform data before motor shaft change is gone. Additionally, the periodic activity that was seen at about 1,000 Hz in low-frequency spectra data before motor shaft change is also now absent. The most obvious change between the two sets of data is the significant increase in the vibration waveform amplitude. The peak-to-peak waveform in the low-frequency data went from 14 g's peak-to-peak to 40 g's peak-to-peak. A similar change occurred in the high-frequency rectified waveform. This is probably because the torsional stiffness increased with the tightening of the system at the motor shaft/key thereby increasing the torsional resonance frequency. The increase in vibration is more desirable than the shaft/key interaction.

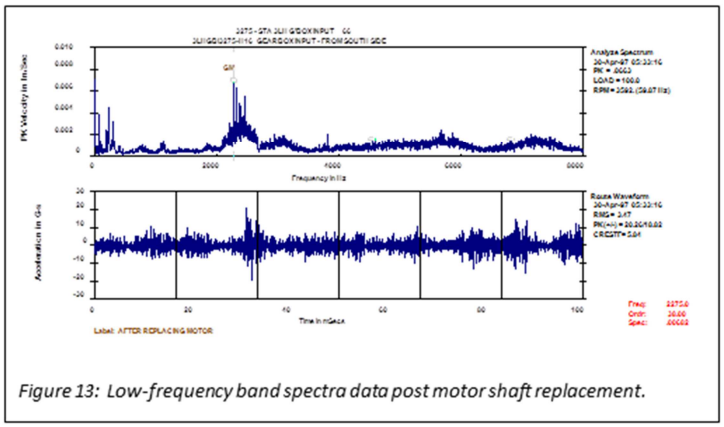

Figure 13: Low-frequency band spectra data post motor shaft replacement.

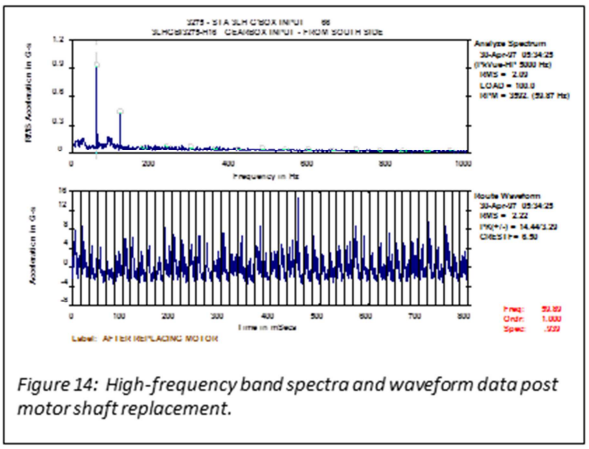

Figure 14: High-frequency band spectra and waveform data post motor shaft replacement.

SECTION 4: CRUSHER GEARBOX

This is a large gearbox measuring roughly 8 x 10 x 20 ft used for crushing rocks at a mining facility. A plan view of the gearbox is presented in Figure 15. There are twelve vibration-monitoring points identified in Figure 15 as 1 through 12 which are used for scheduled acquisition of vibration data.

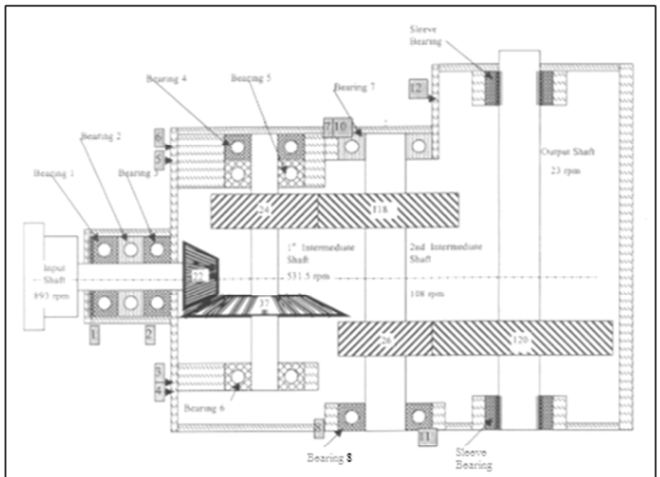

Figure 15: Plan view of crusher gearbox. The input shaft is turning at 893 RPM. The output shaft is turning at 23 RPM. The output shaft is equipped with sleeve bearings. All other bearings are rolling element bearings.

Routine monthly vibration data was acquired from all the measurements points on the gearbox. The high-frequency spectra data and rectified waveform from measurement point #2 are presented in Figure 16. The high-frequency band is from 1 kHz to 40 kHz. The 1 kHz is well above 2.25 times gear mesh frequency. (Gear mesh frequency is 330 Hz, which equals running speed of motor [15 Hz] times the number of teeth [22]). The bearing has an inner race fault in the early stages of failure based on relatively low peak g-level of 3.6 g's. The measurement was repeated approximately one month later and results are presented in Figure 17. The big difference in Figures 16 and 17 is the peak g-level has increased from 3.6 g's to 51 g's, which is significant. This bearing, based on high g-level of 51 g's, requires frequent monitoring with a replacement plan set in motion.

To assure the faulty bearing was bearing #3 and not bearing #1 or bearing #2, data was acquired from measurement point #1 at same time as the data in Figure 17 was acquired. The peak g-level in the high-frequency data from measurement point # 1 was 25 g's versus the 54 g's from measurement point #2. The defective bearing was concluded to be bearing #3. Frequent monitoring with the sensor set on measurement point #2 was then carried out. The peak g-level trend is presented in Figure 18. From the time the 50 g peak level was detected, it took about 25 days to get the bearing replaced. A picture of the defective bearing is presented in Figure 19. The peak g-level recorded was about 80 g's.

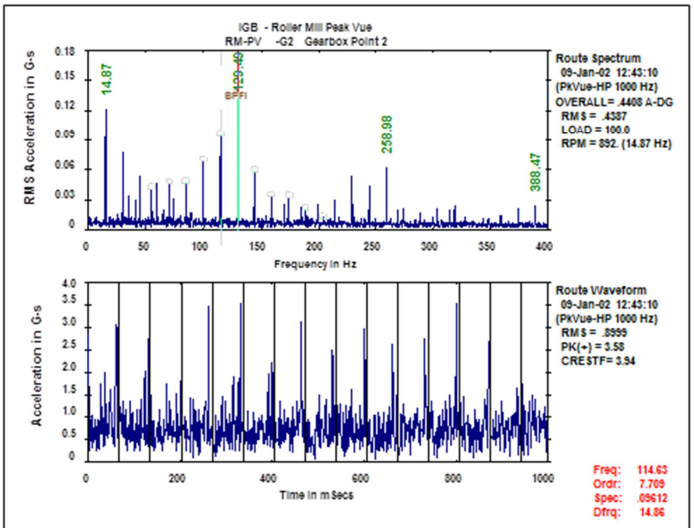

Figure 16: High-frequency, band-rectified waveform and spectra data taken on measurement point 2. Maximum peak g-level in waveform data is 3.6 g's.

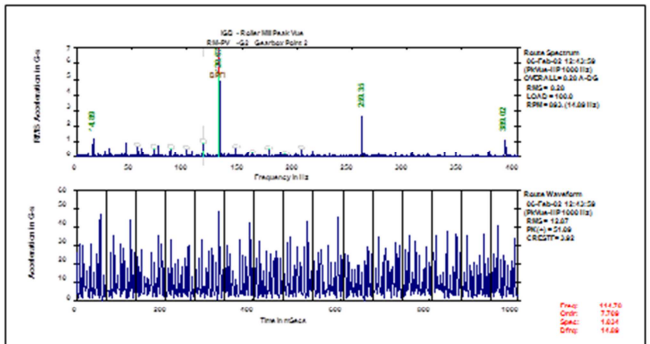

Figure 17: High-frequency, band-rectified waveform and spectra data taken on measurement point 2 one month after the data taken and presented in Figure 16. The peak g-level in waveform data is 51 g's.

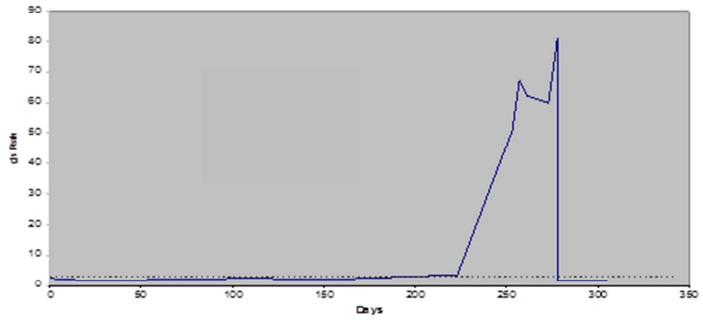

Figure 18: Peak g-level trend over an approximate 300-day monitoring period on measurement point #2.

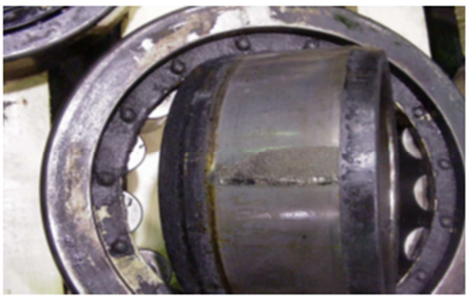

Figure 19: Picture of the defective bearing showing inner race fault. This fault could have been introduced from bearing being stored in vertical position too long. Notice metal removal on inner race downstream of fault suggesting the rolling element was penetrating the oil film when jumping over the crack.

SECTION 5: PRECISION TENSION BRIDLE GEARBOX

A plan view of a precision tension bridle gearbox is presented in Figure 20. The gearbox has a single shaft input with a dual shaft output that ultimately drives the work rolls. The low-frequency and high-frequency band spectra and waveform data were taken with sensor placed over bearing at input to gearbox. The low-frequency band data is presented in Figure 21. The input gear mesh frequency (approximately 351 Hz with second harmonic) is being modulated. The lower gear mesh frequency (approximately 202 Hz) for the 90-tooth gear set is sharp (no indication of modulation) and the second harmonic is not discernible. The rectified waveform and spectra data for the high-frequency band of data from 0.5 to 40 kHz are presented in Figure 22.

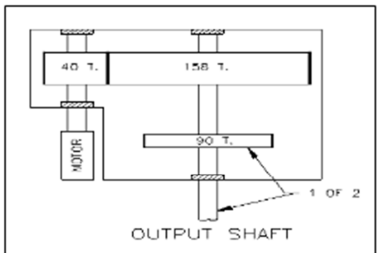

Figure 20: Plan view of the precision tension bridle gearbox.

The spectra data indicates a significant event is occurring once per output shaft revolution. The waveform clearly demonstrates there are two distinct impulses per turn that could mean there are two cracks on one gear. When inspected, two cracked teeth on one gear were found.

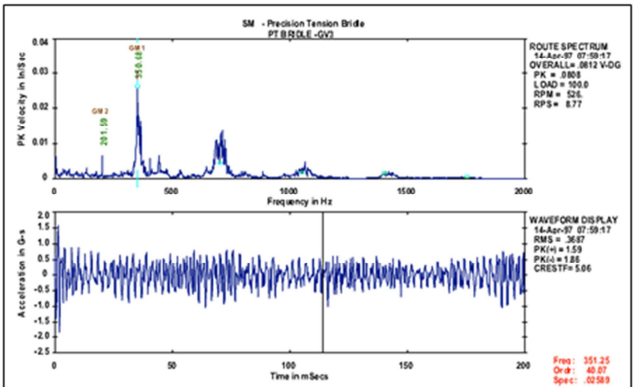

Figure 21: Low-frequency band spectra and waveform data taken from input shaft bearing housing. The most activity is from first and second harmonic of the input gear mesh frequency.

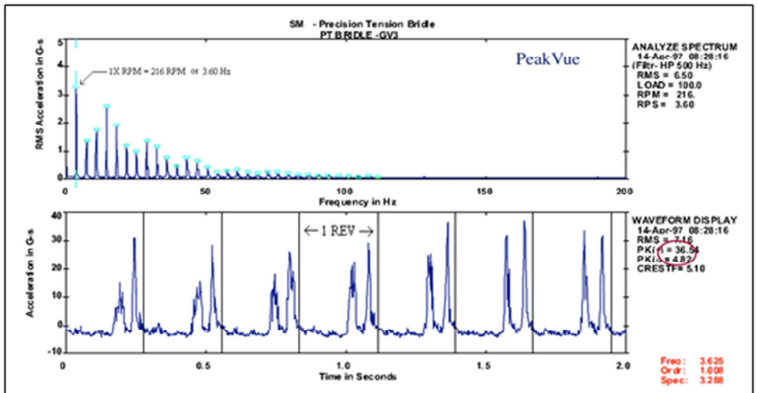

Figure 22: High-frequency band from 0.5 to 40kHz rectified waveform and spectra data. The '1 REV' is for the slow dual shafts output. The spikes occurring once per revolution imply one of the 90 tooth gears has two cracked teeth.

SECTION 6: POST REBUILT GEARBOX WITH CRACKED TOOTH

A gearbox was removed from a mining machine and sent back to the shop for rebuild. A plan view of the gearbox is presented in Figure 23. This gearbox has four gear mesh frequencies. After the rebuild, the machine was subjected to vibration analysis for high and low-frequency bands prior to sending it back to the field. The vibration analyses are carried out on the twelve measurement points (as needed) identified on the gearbox as points G1 through G12. There is a measurement point placed over each bearing. In this case, focus is directed to the low-frequency band up to 1.5 kHz and the high-frequency band from 1 kHz to 40 kHz data from measurement point G5.

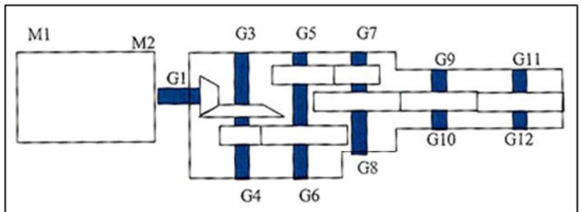

Figure 23: Plan view of rebuilt gearbox prior to sending back to be placed in mining machine.

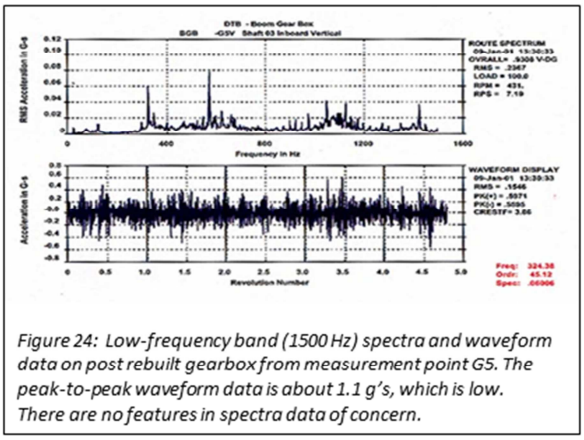

Figure 24: Low-frequency band (1500 Hz) spectra and waveform data on post rebuilt gearbox from measurement point G5. The peak-to-peak waveform data is about 1.1 g's, which is low. There are no features in spectra data of concern.

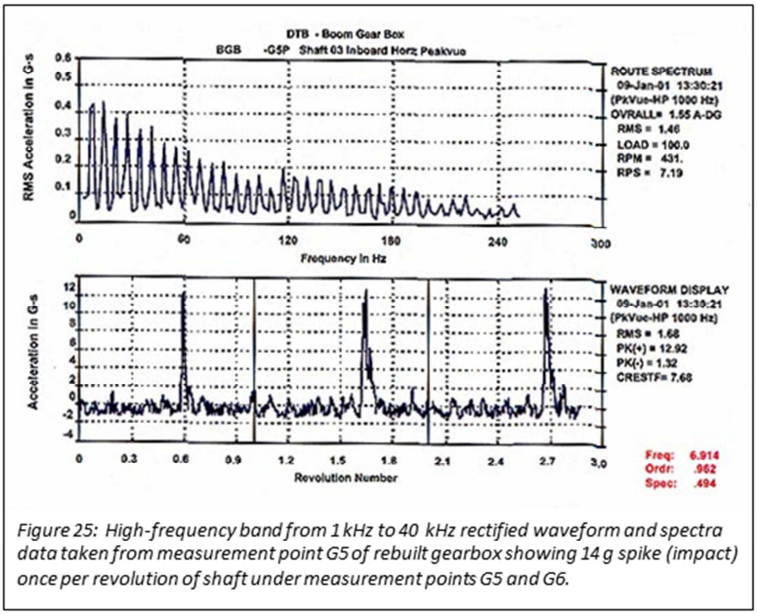

Figure 25: High-frequency band from 1 kHz to 40 kHz rectified waveform and spectra data taken from measurement point G5 of rebuilt gearbox showing 14 g spike (impact) once per revolution of shaft under measurement points G5 and G6.

The waveform and spectra data for the low-frequency band are presented in Figure 24. The peak-to-peak g-level in the waveform data is about 1.1g's, which is not considered to be indicative of a problem. The high-frequency band rectified waveform and spectra data are presented in Figure 25. There is a spike (about 14 g's) occurring once per revolution of the shaft immediately below measurement points G5 and G6. This is the expected signature from a cracked tooth in the gear immediately below measurement point G5. Upon inspection of this gear, it was found to have a crack in the root.

SECTION 7: POST REBUILT GEARBOX WITH ECCENTRIC GEAR

A gearbox was removed from service and sent to the shop for rebuild. Upon completion of the rebuild, the gearbox was subjected to low and high-frequency vibration analysis. The low-frequency measurement showed no sign of a problem. The high-frequency band (from 0.5 to 40 kHz) rectified waveform and spectra data are shown in Figure 26. The high-frequency (0.5 to 40 kHz) rectified waveform is showing a definite repeating pattern of increased activity over approximately 65% of a single revolution

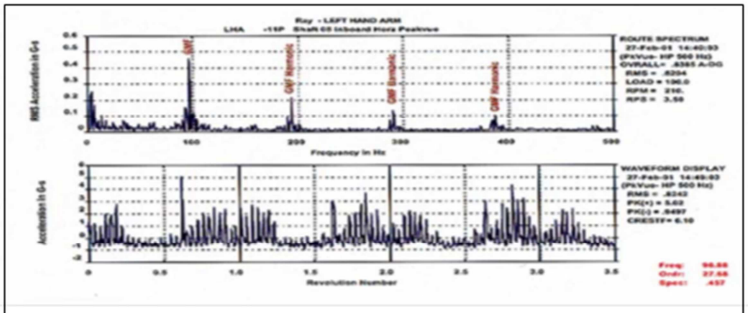

Figure 26: High-frequency band rectified waveform and spectra data from a completed rebuilt gearbox.

and low amplitude activity over the remaining 35% of the revolution. This is the pattern expected for an eccentric gear. In the spectra data, there is significant activity at gear mesh frequency, which is indicative of a stable rotational speed of the gear. Following replacement of the eccentric gear, the high-frequency rectified waveform and spectra were acquired and are presented in Figure 27. Someone was not convinced the gear was eccentric and placed the defective gear in another gearbox. When it was subjected to testing, the results presented in Figure 28 were obtained which was basically the same as that presented in Figure 26.

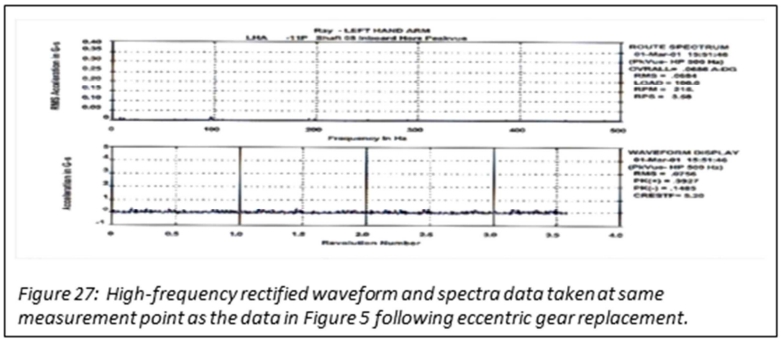

Figure 27: High-frequency rectified waveform and spectra data taken at same measurement point as the data in Figure 5 following eccentric gear replacement.

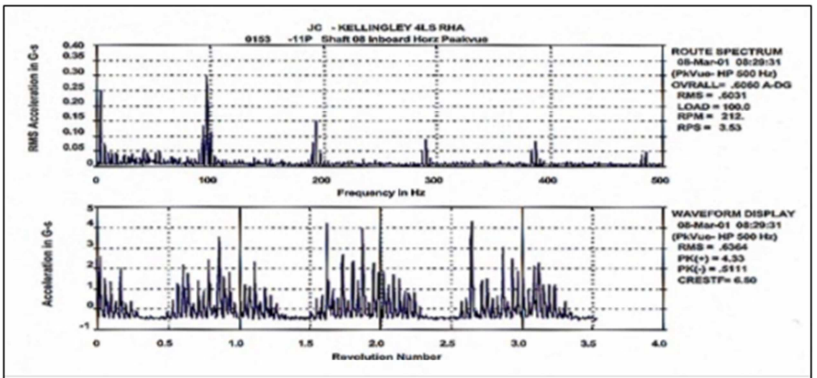

Figure 28: One observer did not believe the gear removed from the machine was eccentric. He proceeded to place the same gear (judged eccentric by many) into a different machine. The data in figure 27 is from that machine.

SECTION 8: FATIGUING IN BEARINGS AND GEARS

Many failures in bearings and gears are initiated by residual stress building up in the metal (e.g., bearings or gears) under usage. When the sum of residual stress and current usage stress exceeds certain levels, the residual stress will be relieved by cracks (fatiguing) starting beneath the surface and proceeding to the outer surface as the cracking progresses under use. When stress relief cracks are initiated, they are accompanied with the emission of stress wave packets that travel at the speed of sound in the material to the outer edge of the component and away from the initiation site. The frequency within the packets is similar to packets emitted when friction occurs (ie.

higher frequencies than when impacting occurs). To illustrate this type of failure, a case from a 1.5 MW wind turbine generator gearbox has been chosen for illustration. The gearbox is made up of a three-wheel planetary gear section driving a two-stage spur gear section. Both sections were housed in a compact housing. An online continuous vibration monitoring system was monitoring the gearbox.

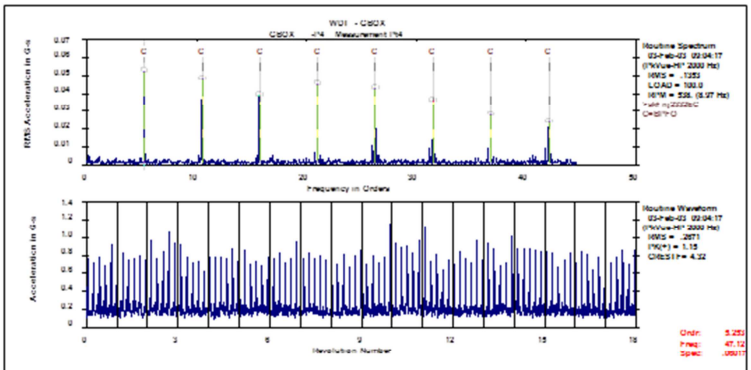

Figure 29: High-frequency rectified waveform and spectra data showing outer race bearing fault (sensor was placed on outer surface of gearbox in vicinity of the bearing.

The rectified high-frequency band (2-40 kHz) waveform and spectra data are presented in Figure 29 from a sensor mounted over the outboard spur section of the gearbox. The spectra data is dominated by activity at 5.253 orders with many harmonics. This is the outer race fault frequency for the bearing used on the outboard end of the intermediate shaft in the spur gear section. The observed peak g-level of 1.15 g's for this speed shaft (538 RPM) is very low. The recommended alert level is 4-5 g's. This fault could very well be from the early stage fatiguing with cracking occurring under the outer race surface. The fault may not be visible if examined at this time by sight or by feel. Typically, wait until peak g-level reaches 6-8 g's (for this speed machine) before a plan is put in place for changing out the bearing unless there are special circumstances such as it is most economical to implement the change at this time.

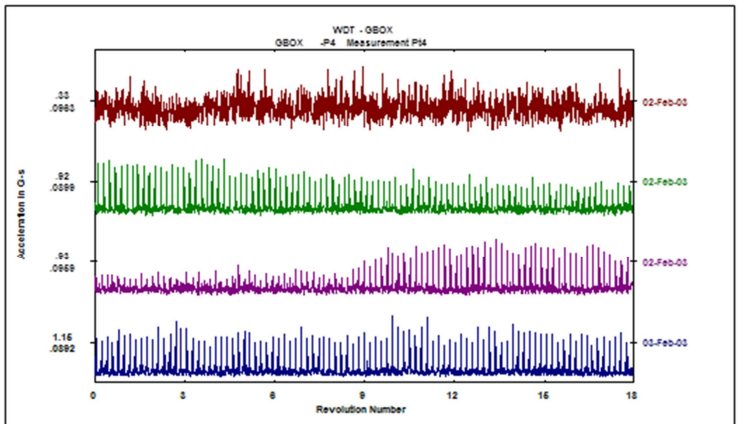

Figure 30: High-frequency, band-limited (2-40 kHz) rectified waveform acquired at different times. Each block of data is 2 seconds (18 revolutions).

The data in Figure 30 was chosen to illustrate how the fault signature can vary over reasonably short times. Each rectified time waveform is for a period encompassing 18 revolutions (2 seconds) of the intermediate shaft turning at 538 rpm. The last trace of data in Figure 30 is the same set of rectified waveform data presented in Figure 29. The three remaining data traces were acquired one day previous.

There is very little fault signature showing up in the first rectified waveform data. In the middle two traces of rectified waveform data, a fault signature is present but with considerable variability. If the signature was a result of impacting from a defect in the inner surface of the outer race, the rectified time waveform would not be expected to have the variability seen in Figure 29.

SECTION 9: CONCLUSIONS

Several faults common to gearboxes were presented in this paper. The objectives were to:

- Demonstrate a wide variation in fault types.
- Demonstrate the importance of employing proper sensors and analysis tools.

Many faults generate a short burst of stress wave activity (from impacting and friction) that requires sensors responsive up to 15-25 kHz, such as IMI Model 603C01. The sensor frequency response is strongly dependent on how the sensor is attached to the surface of the machine. Accelerometer mounting by stud, by flat magnet on a

flat smooth surface and by dual-rail magnet on a curved surface (smooth, rough or painted) were all considered. The conclusion was that the stud-mounting technique was the preferred choice. Mounting the accelerometer with a flat magnet attached to a smooth, flat surface provided sufficient bandwidth for impacting and friction detection. The use of a two-rail magnet on a curved surface would miss several situations where impacting and friction was occurring.

The analysis tools used in this study consisted of the normal spectra data in velocity units and waveform in acceleration units. To cover the high frequency burst of stress waves from impacting, friction and fatiguing, the waveform used was the band-limited rectified signal. The band-limited rectified signal was 0.5-40 kHz, 1.0-40 kHz or 2.0-40 kHz. The rectified waveform was also transformed to spectra data in acceleration units. In addition to waveform and spectra data, the autocorrelation coefficient data was computed from the waveform data graphically displaced. It was a very useful diagnostic tool in both fault identification and severity assessment.

IMI SENSORS
A PCB PIEZOTRONICS DIV.

3425 Walden Avenue, Depew, NY 14043-2495 USA

Toll-Free in the USA: **800.959.4464** | 24-hour SensorLine[SM]: **716.684.0003**

Fax: **716.684.0987** | Email: **info@pcb.com**

| VISIT US AT WWW.PCB.COM/IMI-SENSORS |

IMI SENSORS designs and manufactures a full line of accelerometers, sensors, vibration switches, vibration transmitters, cables and accessories for predictive maintenance, continuous vibration monitoring, and machinery equipment protection. Products include rugged industrial ICP® accelerometers, 4-20 mA industrial vibration sensors and transmitters for 24/7 monitoring, electronic and mechanical vibration switches, the patented Bearing Fault Detector, high temperature accelerometers to +1300 °F (+704 °C), 2-wire Smart Vibration Switch, and the patented Reciprocating Machinery Protector. CE approved and intrinsically safe versions are available for most products.

THE INDUSTRY'S ONLY COMMITMENT TO TOTAL CUSTOMER SATISFACTION.